Article

Antimicrobial effect of nano-silver against oral Streptococci: implications in containment of bacterial biofilm on orthodontal appliances

Saba farheen[1†], Abdul M Oanz[1†], Nazoora Khan[1†], Mohd Saad Umar[1], Fauzia Jamal[1], Mohammad Kashif[2], Ansam Wadia Alshameri[1], Saba Khan*[3], Mohammad Owais*[1]

****

[†]These authors contributed equally to this work,

[1]Interdisciplinary Biotechnology Unit, Aligarh Muslim University, Aligarh-202002, INDIA,

[2]CSIR-NBRI, Lucknow-226001,

[3]Department of Orthodontics, Dental College, Aligarh Muslim University, Aligarh-202002, INDIA,

[*]Correspondence at: Interdisciplinary Biotechnology Unit, Aligarh Muslim University, Aligarh-202002, INDIA,

 doi:10.20944/preprints202102.0436.v1

Abstract

Among various metal-based nanoparticles, silver nanoparticles (AgNPs) manifest superior inhibitory effect against several microorganisms. In fact, the AgNPs based therapy has been reported to inhibit both sensitive as well resistant isolates of bacteria and other disease causing microbes with equal propensity. Keeping this fact into consideration, we executed bio-mediated synthesis of AgNPs employing *Hibiscus rosa sinensis* flower extract. The as-synthesized AgNPs were evaluated for their potential to inhibit *Streptococcus mutans* (*S. mutans*), one of the main causative bacteria for dental caries. Beside several other reasons, orthodontic appliances have also been reported to facilitate infliction of oral cavity with a range of microbes including *S. mutans*. To determine the growth inhibitory and anti-adherence activity of AgNPs on orthodontic appliance, we performed microbiological assays employing AgNPs adsorbed on to the orthodontic wires. Topographic analysis of orthodontic wires was executed by scanning electron microscopy. In addition to antimicrobial and antibiofilm activity against oral *S. mutans*, the as-fabricated AgNPs demonstrated significant inhibitory and anti-biofilm properties against other biofilm forming bacteria such as *Escherichia coli* and *Listeria monocytogenes* as well.

Key word: silver nanoparticles, biofilm, orthodontic wire, drug resistance, oral-*Streptococcus*

Preprints (www.preprints.org) | NOT PEER-REVIEWED | Posted: 19 February 2021 doi:10.20944/preprints202102.0436.v1

1. Introduction

The nano-sized metal particles exhibit altered chemical and physical attributes as compared to their precursor chemical entities. Considering this fact, there has been an increasing trend in exploitation of metal-based nano-particles in diversified fields ranging from optics, catalysis as well as in medical diagnostics and therapeutics *etc* [1-3]. Well-dispersed and ultrafine metal nano-particles acquire distinctive thermodynamic properties when compared to their precursor metal compounds. Because of their nano order size dimensions, high energy surface atoms, greater penetration and ability to target various vital biological molecules of the host, the nano-particles have been widely used in various medical science related fields as well [2, 3].

It is noteworthy that the nanometer size of the particles renders them the ability to traverse various biological barriers of the recipient's body and even guide them to accumulate in tissues either beneath the skin or deeper into the organs like lungs, liver and even less accessible component of CNS such as brain [4]. As a consequence, the NP based drug delivery systems have been widely exploited in treatment of cancer and several infectious diseases as well [5].

Various chemical and physical methods such as UV or microwave irradiation, chemical reduction, photochemical process, electron irradiation *etc*., have been widely used in the synthesis of nano-particles [6]. Most of these methods involve multistep processing, requirement of high energy input or involvement of hazardous chemicals to carry on NP synthesis. Moreover, most of the above-mentioned methods require relatively sophisticated instrument for NP synthesis and also suffer from the limitations such as low material conversion and difficulty in purification *etc*. On a positive note, there has been a sudden shift in the focus of scientific community towards exploitation of plants and their extracts as reducing cum stabilizing agents and their usage in the synthesis of metallic nano-particles. The 'green synthesis' approach has been receiving increased attention as it is environment friendly and causes almost negligible pollution of any kind [7]. Further, the cost effective green synthesis technique has edge over other synthesis methods and can be easily modulated for large scale production [8]. Moreover, by smart maneuvering of fabrication conditions, green method can be manipulated to synthesize nano-particles with diverse shapes and range of sizes [7, 8].

Preprints (www.preprints.org) | NOT PEER-REVIEWED | Posted: 19 February 2021 doi:10.20944/preprints202102.0436.v1

Dental caries, a multi-factorial disease, has been considered as a serious oral health issue. It is more common in individuals, who wear orthodontic appliances. The orthodontic devices not only offer a platform to growing microbes, however, pose an obstacle in biofilm removal during oral hygiene procedures. The disease leads to demineralization and erosion of the tooth enamel surface. Prolonged dental plaque facilitates accumulation of *Streptococcus mutans (S. mutans)*, the causative oral pathogen, that in turn ensues in development of dental caries [9]. Moreover, various orthodontic elastomeric modules, including brackets and wires, when accompanied with poor oral hygiene may also lead to establishment of infection caused by various oral bacteria such as *S. mutans* [10]. The bacterial infection is generally accompanied with formation of biofilm on both tooth enamel as well as orthodontic appliances used in dental care setup [11]. The related oral clinical issues may result in unacceptable esthetic presentation. If not treated properly, the infection not only causes bacteremia, however, also accompanied with inflammatory response in the afflicted patients. The infection may lead to infective endocarditis as well [12]. Among various metal-based nano-particles, silver nano-particles possess excellent antimicrobial property against wide range of microorganisms. The special treatment of orthodontic appliances with NPs, before their usage in clinical settings, is likely to combat invading pathogens by manifesting strong anti-biofilm activity [13].

Hibiscus rosa-sinensis Linn (Family Malvaceae) is reported to possess potent medicinal properties including antitumor, cardio- protective, hypotensive, antidiabetic, anticonvulsant wound and antioxidant activity [14]. The *Hibiscus rosa-sinensis* flowers (*HRSF*) are known to contain flavonoids like anthocyanin and quercetin. The *HRSF* flavonoids have also been implicated for their anti-depressant and anxiolytic activity [15].

In the present study, we first ascertained the potential of a novel *HRSF* extract to synthesize silver nano-particles. The characterization of as-synthesized silver nano-particles (AgNPs) revealed that in a manner similar to other plant or bacterial exudates, HRSF extract too has potential to facilitate fabrication of nanosized particles in a time and concentration dependent manner. The kinetics of as-synthesized AgNPs synthesis was monitored employing UV spectrophotometry. The resultant NPs were characterized using various spectroscopic techniques. The antibacterial and anti-biofilm potential of as-formed AgNPs was evaluated against range of bacteria including caries causing *S. mutans*. Further, we also assessed anti-adherence potential of AgNPs against *S. mutans* adsorbed on orthodontic wires.

Preprints (www.preprints.org) | NOT PEER-REVIEWED | Posted: 19 February 2021 doi:10.20944/preprints202102.0436.v1

2. Material and methods

Hibiscus rosa-sinensis* flower extract preparation**. Fresh flowers of ***Hibiscus rosa-sinensis were collected and washed several times with deionised water. A known volume of distilled water **(**100 ml) was mixed with 10g (wet weight) of thoroughly washed *HRS* flowers. The mixture was boiled till the original volume of aqueous suspension reduced to 50ml and filtered through a Whatman No. 1 filter paper. The resulting HRSF extract was used in synthesis of as-fabricated AgNPs.

Synthesis of AgNPs using *HRS* flower extract. Increasing volumes (3-5 ml) of *HRSF* extract were added to 5ml aqueous solution [10^{-3} M] of silver nitrate. The final volume of each of the reaction mixture was made up to 10ml by adding sufficient amount of distilled water and was kept on stirrer for overnight. The as-formed nano-particles were characterized by various spectro-photometric, transmission electron microscopy (TEM) and DLS based analyses.

UV absorbance spectroscopic studies. UV spectroscopic analysis of the as-synthesized nanoparticles was done to ascertain biogenic reduction of precursor silver nitrate salt. The double beam spectrophotometer (Jasco model V-750), operated at a resolution of 1 nm, was used to execute analysis (8). The UV–VIS spectra was recorded over the 200–800 nm range.

Fourier transform infrared spectroscopy (FT-IR) measurement. FT-IR of as-formed AgNPs was analyzed on Perkin-Elmer FT-IR spectrophotometer in the diffuse reflectance mode operating at a resolution of 4 cm^{-1} (9). The samples were run in triplicate to validate the readings. The spectra were taken between 4000 cm^{-1} and 500 cm^{-1} by averaging 128 cm scans for each spectrum.

Transmission Electron Microscopy (TEM) Measurement. The as-formed AgNPs, synthesized with the help of *HRSF* extract, were characterized by TEM. We also studied effect of increasing volumes of *HRSF* extract on the shape and size of the as-formed AgNPs with the help of JEOL transmission electron microscope at an accelerating voltage of 200 kV. A copper grid mesh, covered with the carbon-stabilized film was employed to analyze the as-synthesized AgNPs. The uranyl acetate (2%w/v) solution was used for negative staining of the sample.

Zeta-potential determination. For the determination of Zeta-potential of as-synthesized AgNPs, DTS software, which was based on M3-PALS technology (Malvern Instrument

Preprints (www.preprints.org) | NOT PEER-REVIEWED | Posted: 19 February 2021 doi:10.20944/preprints202102.0436.v1

Limited, UK), was used. Reconstitution of the samples was done in 5 mM phosphate buffer, pH 7.4 and the electrophoretic mobility was measured in the electrophoresis cell. The sample was run in triplicate to determine the zeta potential.

Anti-bacterial potential of as-synthesized AgNPs as revealed by zone of Inhibition assay

The bactericidal activity of the as-formed AgNPs was assessed employing agar well diffusion method. Various bacterial strains such as *Listeria monocytogenes, S. mutans* and *Escherichia coli* were used in the study. The bacterial strain *S. mutans* MTCC 497 (Institute of Microbial Technology, Chandigarh, India) was cultured in Brain Heart Infusion (BHI) Broth (Himedia Labs, Mumbai, India) at 37°C. *S. mutans* MTCC497 was resistant to ampicillin, azithromycin, ceftriaxone and vancomycin. We also used a *S. mutans* serotype c strain (ATCC 700610 /UA159) to assess antibacterial potential of as-formed AgNPs. This strain was sensitive to erythromycin, rifampin, rifampicin, rifamycin and streptomycin *etc* in our hand. Next, we determined antibacterial potential of as-synthesized AgNPs against standard *E. coli* (ATCC-25922). The antibacterial potential of as-synthesized AgNPs was also established against *L. monocytogenes* ATCC 19115 and *L. monocytogenes* MTCC 839. The clinical isolates of *S. mutans*, used in the study, were kind gift of Prof. Shahid from Deptt. Of Microbiology, JNMC, AMU, Aligarh.

Nutrient broth was used for sub culturing of the pure culture of *S. mutans, E.coli and L. monocytogenes*. They were grown overnight to attain the colony-forming unit (CFU) counts of $\sim 10^6$ units per ml. An aliquot of 100µl, from overnight grown culture, was spread uniformly on nutrient agar petri-plate by sterile plastic spreader.

The agar plate, inoculated with S. *mutans*, was co-cultured with AgNPs Ni-Ti orthodontic wire. The uncoated as well as plain $AgNO_3$ coated Ni-Ti orthodontic wires were used as control. The plates were incubated at 37 °C and the zone of inhibition was observed after the stipulated time period of 24hrs.

In the next set of experiment, the agar plates were first exposed with *E. coli* and *L. monocytogenes* followed by boring of the wells using punching machine. Subsequently, an increasing amount of as-synthesized AgNPs (1 mg/ml stock solution) or standard antibiotic, gentamicin (control) was dispensed into the various wells in a given agar plate. The plates were incubated at 37 °C and the zone of inhibition was determined by measuring the clear region around each well after the stipulated time period of 24hrs.

Preprints (www.preprints.org) | NOT PEER-REVIEWED | Posted: 19 February 2021 doi:10.20944/preprints202102.0436.v1

Antibiofilm potential of as-synthesized AgNPs employing XTT assay

The anti-biofilm potential of as-synthesized AgNPs was established employing XTT assay following published protocols with minor changes as standardized in our lab. Briefly, 100 µl of bacterial cell culture ($1x10^8$ cells/ml) was dispensed in each well of 96 well culture plates. The bacteria were allowed to form adherent mature biofilm in the presence of increasing concentration of the as-formed AgNPs for 48hrs. Just before the commencement of the assay, a solution of Menadione (0.4 mM) was prepared and filtered.

The plate was incubated for stipulated time period, followed by washing with PBS (200ul). Next, XTT reagent [2, 3-Bis (2-methoxy-4-Nitro-5-sulfophenyl) -5-{phenylamino} carbonyl) -2H-tetrazolium hydroxide (XTT) at a final concentration of 250 µg/ml] was dispensed to each test well of the plate followed by addition of menadione solution (2 µl/well). The plate was further incubated for the next 4hrs at 37 °C in the dark. Next, the solution was transferred into a fresh plate to assess the colorimetric change using a microtitre plate reader (BIORAD Microplate reader at 490 nm). The XTT experiments were performed in triplicate to validate the data.

Effect of as-synthesized AgNPs on the adherence of *S. mutans* to Smooth Glass Surfaces in presence of sucrose

We studied effect of as-synthesized AgNPs on the adherence of *S. mutans* on smooth glass surface. We also assessed effect of presence of sucrose in the surrounding medium during AgNP mediated inhibition of *S. mutans* adherence. The bacteria were cultured at 37 °C for 24 h at an angle of 30° in a glass tube containing 10 ml of BHI with or without 5% (w/v) sucrose. The cultured tubes were also exposed with the sub-MIC concentrations of the AgNPs. The culture medium was consisting of BHI with (sucrose dependent) and without sucrose (sucrose independent). After stipulated incubation, the glass tubes were slightly rotated to decant the planktonic cells. Subsequently, the adhered cells were removed by adding 0.5 M of sodium hydroxide with stirring. The cells were thoroughly washed and suspended in saline. The adherence was determined spectrophotometrically at 600 nm. The percentage adherence was determined by using formula:

Percentage adherence = (O.D. of adhered cells/O.D. of total cells) ×100.

Preprints (www.preprints.org) | NOT PEER-REVIEWED | Posted: 19 February 2021 doi:10.20944/preprints202102.0436.v1

The effect of AgNPs on the cell surface hydrophobicity of *S. mutans* was determined by measuring its adhesion with hydrocarbon. The cells were grown in BHI medium supplemented with 5% sucrose along with increasing concentration AgNPs. The cells were washed twice and suspended in sterile saline (0.85%) to adjust optical density (O.D.) at around 0.3 at 600 nm.a given volume of the cell suspension (3 ml) was mixed with 0.25 ml of toluene. The tubes were stirred for 2 min and allowed to equilibrate at room temperature for 10 min. The cell suspension was kept aside to allow phase separation. We next determined the O.D. of the aqueous phase spectrophotometrically at 600 nm.

Hydrophobicity index of as-synthesized AgNPs treated bacterial biofilm

Overnight cultured bacterial cells (treated and control) were suspended in 1 ml LB medium to obtain optical density (at wavelength of 595nm) at around 1.0 ± 0.01. Further, toluene (1ml) was added to the suspension (both treated and control) and vortexed. The test tubes were incubated for 30 mins to let the biphasic solution to settle. Next, the optical density of the aqueous phase was measured and the hydrophobicity index was calculated by using the equation:

$$HI\ \% = [(Ai - Af)/Ai] \times 100$$

Where Ai and Af denote the initial and final optical densities of aqueous phase. The adherence of the bacterial cells to the organic solvent was evaluated to ascertain the hydrophobicity [16].

Anti-adherence properties of as-synthesized AgNPs

Sterilized Ni-Ti orthodontic wires were placed into three separate Eppendorf tubes, having fresh sterilized nutrient broth. Next, one of the two sets of orthodontic wires was co-incubated with as-synthesized AgNPs and other with aqueous $AgNO_3$ solution. The wire, incubated in media only, served as control. Standardized suspension ($1x10^8$ cells/ml) of *S. mutans* was added to each Eppendorf tube (harboring orthodontic wire) and was incubated for 24 hrs at 37°C. Once the incubation period was over, wires were taken out and placed into fresh Eppendorf tubes containing PBS and subjected to sonication to remove adhered bacteria from wires. A known volume (100 ul) of the resultant bacterial suspension (diluted 100 times), collected post sonication was spread on a NB agar plate and incubated for 24 hrs at 37 °C and CFU/ml was calculated for each group.

Preprints (www.preprints.org) | NOT PEER-REVIEWED | Posted: 19 February 2021 doi:10.20944/preprints202102.0436.v1

Anti-Biofilm activity as revealed by fluorescence microscopy.

S. mutans biofilm, cultured on sterile glass cover slip, was placed in the well of multi-well polystyrene plate. Briefly, *S. mutans* cell suspension (at the 1.0 absorbance $O.D_{600}$ in NB medium) was cultures on a coverslip overnight at 37°C. After 24h incubation, media was replenished and biofilm was exposed to AgNPs suspension for duration of 3 hrs. Untreated mature biofilm was considered as control. After treatment with AgNPs and aqueous $AgNO_3$solution, the plate was washed with PBS, and the anti-biofilm activity was observed by fluorescence microscopy.

Quantification of extracellular glucan in cultures with sucrose

The phenol/H_2SO_4 method was used to quantify the glucan in the cultured sample. *S. mutans* was incubated in media containing 1% sucrose both in absence and presence of as-synthesized AgNPs for 20 h, after which the bacteria were recovered. Extracellular water-soluble glucan was isolated by employing ethanol-precipitation of the supernatants from the recovered bacterial cultures. The remaining cell pellet was re-suspended in 1 M NaOH and centrifuged to remove bacterial cells. Water-insoluble glucan was recovered by ethanol-precipitation of the supernatant.

Assessment of topographical changes in orthodontic wires

Ni-Ti orthodontic wires were incubated with as-synthesized AgNPs and aqueous $AgNO_3$ for 24 hrs with mild and continuous shaking for homogenous adherence. Topographical changes on coated Ni- Ti orthodontic wires as compared to uncoated one (control) were assessed by Scanning Electron Microscopy.

3. Results

***Hibiscus* flower extract mediated synthesis of metal nanoparticles**

The potential of HRSF extract to synthesize nano particles was established by evaluating its ability to convert silver salt to as-synthesized silver nanoparticles. The aqueous silver ions were exposed to the HRS flower extract. The color of the reaction mixture changed from pale yellow to blackish grey. The color transformation corresponds to characteristic surface plasmon resonance (SPR) effect of different sized silver nanoparticles. SPR analysis establishes HRSF mediated synthesis of Ag NPs.

Preprints (www.preprints.org) | NOT PEER-REVIEWED | Posted: 19 February 2021 doi:10.20944/preprints202102.0436.v1

UV-VIS spectra of silver nanoparticles

The optical properties of the as-formed AgNPs were determined employing surface plasmon absorption spectroscopy. The SPR properties usually depend on the shape of NP population. At the outset, a UV–visible absorption spectroscopic technique was used to analyze the synthesis of the nanoparticles. Figure 1A shows the UV–VIS absorption spectra recorded for as-synthesized silver nanoparticles harvested after 24 hrs of reaction (upon treatment with 3ml of *HRSF* extract). The results indicate that the reaction solution displays an absorption maximum at about 480 nm that can be attributed to the SPR of the as-formed silvernanoparticles [17]. It was observed that with increase in time, silver nano-particle synthesis rate also increased (data not shown). Although, the wavelength maximum was stably positioned at 480 nm, however, the intensity steadily increased with the time and eventually got saturated after 24 hrs. The longitudinal plasmon exhibited a change in position with time (data not shown).

We also studied the kinetics of silver nanoparticle synthesis upon incubation of $AgN0_3$ with increasing content of *HRS* flower extract. The synthesis of AgNPs augmented upon increasing the concentration of plant extract in the reaction medium. The increase in HRSF content (3ml vs 5ml *HRSF* extract) resulted in upsurge in absorbance at 480 nm (Figure 1A).

TEM and DLS Analysis

The biomimetic synthesis of silver nano-particles was further confirmed by representative TEM images of silver nanoparticles generated employing increasing amounts of flower extract for their synthesis. The shape of the particles was found to be dependent on the concentration of flower extract. Higher abundance of *HRSF* extract favored the occurrence of large homogenous population of small sized nano particles. At lower concentration of flower extract various triangular and hexagonal and ovoid shape particles in the size range 10-40 nm (Fig 1B) were seen to be coexisting. However, as the concentration of HRSF extract was increased, the average diameter of the silver nanoparticles was found to decrease as evidenced by the occurrence of spherical particles (15-25nm) at higher concentration of HRS flower extract (Figure 1C). Also, as the flower extract concentration increased, the total number of particles in a given volume increased simultaneously as seen in the TEM micrograph (Figure 1C). Initially, the increase in the HRSF extract causes the nanoparticles to be formed in the range of 30-50 nm. This is more evident from the fact that higher

Preprints (www.preprints.org) | NOT PEER-REVIEWED | Posted: 19 February 2021 doi:10.20944/preprints202102.0436.v1

concentration of flower extract led to the synthesis of large number of isomorphic spherical nanoparticles of small dimensions (20-30nm), which is accompanied by decrease in number of large sized compounds with size range of 30-50 nm.

For the determination of particle size of as-synthesized AgNPs in aqueous solutions dynamic light scattering (DLS) analysis was carried out. DLS technique helps in assessment of the size of as-synthesized particles. It also helps in providing information regarding size distribution of the nano-particles as well. To have better information pertaining to size distribution of as-formed AgNPs, DLS is performed in conjunction with TEM analysis. Analysis of the *HRSF* extract-mediated synthesized AgNPs dynamic light scattering (DLS) pattern showed average size of as-formed AgNPs to be around 30-80 nm (Figure 1D). The TEM analysis revealed the morphology of the as-synthesized AgNPs to be spherical/ovoid and a size range of around 30-50nm. The discrepancy in the size as determined by DLS versus TEM analyses is usually explained on the basis of hydrodynamic diameter of AgNPs which correspond to size of the particles suspended in liquid ambiance (Figure 1B &1C).

Surface Charge of AgNPs as measured by Zeta Potential

Zeta potential is a physical property which relates to the net surface charge of the nanoparticles. Depending upon the magnitude and nature of the charge, the particles may repel each other (because of the Coulomb explosion force) that eventually prevent agglomeration of the as-formed nanoparticles. The stability of NPs has been correlated well with the zeta potential ranging from +30 mV to -30 mV. The as-synthesized AgNPs were found to have zeta potential around-25 mV [Figure 1E].

FT-IR analysis

FTIR was used for characterization of resultant silver nano-particles obtained after HRSF extract mediated reduction of silver nitrate. Curve A, of the figure 2, belongs to HRSF extract, curve B represents the aqueous solution of $AgNO_3$, curve C belongs to the as-synthesied AgNPs produced by the reduction of silver nitrate by HRSF extract. The FTIR analysis of HRSF extract (curve A) displayed bands in the region of 3500-3000 and 1680-1500 cm^{-1}. The absorption peak in the region of 3500-3000cm^{-1} is characteristic of the hydroxyl group in phenolic and alcoholic compounds. Curve A also shows charactersitic absorbtion bands at 820-550 cm^{-1} that correspond to -CH group. The FTIR spectrum of as-synthesied AgNPs illstrates more peaks in the region of 3500-3000cm^{-1} due to stretching and

Preprints (www.preprints.org) | NOT PEER-REVIEWED | Posted: 19 February 2021 doi:10.20944/preprints202102.0436.v1

vibrations of hydroxyl group of alcholic and phenolic compounds (Curve C, D) mainly at 3228, 3223 3115, 3154, 3206.90, 3450 and 3486 cm^{-1} (due to vibrations in phenolic compound). The band in the region of 1680-1500cm^{-1} has been shared between amide bond of protein (sourced from flower extract) and also due to stretching vibrations in secondray structure of portein resulting in the formation of peaks at 1632, 1640, 1513, and 1554 cm^{-1} as clearly revealed in curves C and D of silver nanoparticles. FTIR analysis also showed peaks at 1159 and 1111.02cm^{-1} corresponding to comparative shift to the control (HRSF extract, curve A) due to vibration of C=O group. The absorption bands are also observed in the region of 820-550cm^{-1}, which may correspond to the C-H deformations in synthesized silver nanoparticles [Figure 2].

Anti-bacterial potential of AgNPs as assessed by agar well diffusion method

The antimicrobial activity of AgNPs was assessed against *S. mutans*, using the agar well diffusion assay. The zones of inhibition (in mm) around each well containing AgNPs had been assessed (**Figure 3)**. We also determined antibacterial activity of the as-synthesized AgNPs against *E. coli* and *L. monocytogenes*. The AgNPs exhibited significant antibacterial activity against all the tested organisms. Besides inhibiting cell-to-cell interaction, the AgNPs also induced ROS production. This led to fragmentation of DNA. The antibacterial activity of AgNPs can also be attributed to the inhibition and/or disruption of respiratory chain and cell division process that ultimately leads to cell death [18]. The silver nanoparticles have been reported to release silver ions inside the bacterial cells thereby inciting killing of the treated bacteria[19].

Ni-Ti orthodontic wires were coated with as-synthesized AgNPs or $AgNO_3$ solution. The impregnated wires were placed on the agar plate that was previously inoculated with resistant isolates of *S. mutans*. The wire impregnated with AgNPs showed significant *S. mutans* inhibition (clear zone of inhibition) as compared to $AgNO_3$ coated wire (Figure 4).

Anti-adherence potential of as-formed AgNPs

Ni-Ti orthodontic wires (coated with AgNPs or $AgNO_3$) were placed into Eppendorf tubes. The wire harbouring tubes were co-exposed with fresh NB broth along with suspension of less sensitive *S. mutans.* On completion of stipulated incubation period, wires were taken out and placed into fresh Eppendorf tubes containing PBS and subjected to sonication to remove adhered bacteria. The detached bacteria were cultured on agar plate. The wire treated with

Preprints (www.preprints.org) | NOT PEER-REVIEWED | Posted: 19 February 2021 doi:10.20944/preprints202102.0436.v1

AgNPs showed less bacterial load as compared the one that was treated with aqueous $AgNO_3$ solution (Figure 5a and 5b).

Anti-biofilm potential of as-synthesized AgNPs employing XTT assay

The as-synthesized AgNPs inhibited adherence of *S. mutans* to glass tubes. The as-synthesized AgNPs inhibited both sucrose-independent as well as sucrose-dependent adherence of the treated *S. mutans* bacteria. The inhibition was more pronounced in sucrose-dependent adherence as compared to the treated sucrose free medium. The as-synthesized AgNPs inhibited the *S. mutans* biofilm formation in a dose-dependent manner (**Figure 6**A). The AgNPs at a concentration of around 6.25 g/ml inhibited around 50% of the formed biofilm.

AgNPs mediated hydrophobicity inhibition of the treated *Streptococcus mutans*

The as-synthesized AgNPs were found to inhibit cell surface hydrophobicity of the *S. mutans* in a concentration- dependent manner as shown in **figure 6B**. The As-synthesized AgNPs reduced the hydrophobicity to more than 50% at a concentration of ~100 µg/ml.

We also determined anti-biofilm potential of as-synthesized AgNPs against less susceptible isolates of *L. monocytogenes and E. coli*. Increasing amount of AgNPs (ranging from1.56 to 200µg/ml) was dispensed in each well of microtiter plate. Subsequently, the plate was inoculated with a bacterial strain (for 24 h) as specified in method section. It can be inferred from the results that the biologically synthesized AgNPs based formulation was successful in inhibiting the drug resistant bacterial biofilm (less susceptible against gentamycin), as compared to the negative control (Figure S2). The adherence potential of bacterial cells can be attributed to the high hydrophobicity associated with the bacterial cell surface. The percentage of hydrophobicity index for *E. coli* (less susceptible isolate) decreased from ~58% to ~34% on treatment with as-synthesized AgNPs. Similarly, the hydrophobicity index for less susceptible *L. monocytogenes* isolate decreased from ~64 % to ~ 43 % (Figure S2).

Anti-Biofilm activity as revealed by fluorescence microscopy

To ascertain the anti-biofilm potential of the as-formed AgNPs, we assessed *S. mutans* (less susceptible isolate) mediated synthesis of biofilm on glass surface. The fluorescence microscopy reveals formation ofmature biofilm when *S. mutans* was cultured in absence of AgNPs. It could be attributed to unhindered proliferation of untreated cells leading to biofilm

Preprints (www.preprints.org) | NOT PEER-REVIEWED | Posted: 19 February 2021 doi:10.20944/preprints202102.0436.v1

formation. On the other hand, the treatment with AgNPs resulted in the inhibition of biofilm formation on the glass surface [Figure 7].

The as-synthesized AgNPs inhibited glucan synthesis in the treated *S. mutans* cells

We determined potential of the as-synthesized AgNPs to inhibit glucan synthesis in the treated *S. mutans*. The AgNPs efficiently inhibited glucan synthesis in a concentration-dependent manner. The AgNPs inhibited around 50% glucan synthesis at around 100 µg /ml concentration (Figure 6).

Assessment of topographical changes in orthodontic wires

Surface morphology or the topographic conditions of Ni-Ti orthodontic wire was studied by SEM analysis (Figure 8). As revealed by SEM micrographs, the surface of AgNPs coated Ni-Ti orthodontic wires showed less irregular topography in comparison to both $AgNO_3$ solution coated as well as bare wires (no coating). The uncoated Ni-Ti orthodontic wires were found to possess significant number of well-distributed irregular cavities as well as large number of pores on their surface. On the other hand, less topographic irregularities were observed on Ni-Ti wires that were coated with $AgNO_3$ solution.

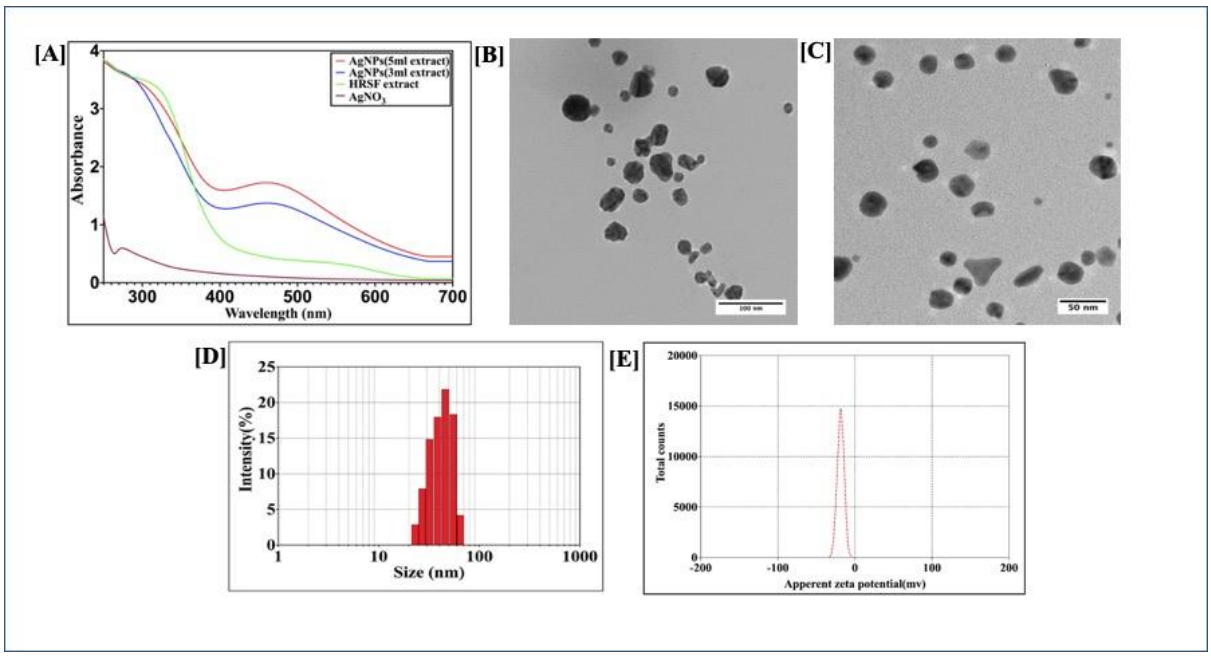

Figure 1

Figure 1. UV–Visible absorption spectrum of as- synthesized AgNPs fabricated with the help of HRSF extract:1A, UV-Visible spectra of silver nanoparticles formed upon incubation of $AgNO_3$ (10^{-3}M) solution with increasing concentrations of HRSF extract. The

Preprints (www.preprints.org) | NOT PEER-REVIEWED | Posted: 19 February 2021 doi:10.20944/preprints202102.0436.v1

characteristic surface plasmon resonance (SPR) bands corresponding to as-formed silver nanoparticles progressively manifest hyperchromic shift toward higher wavelength with accompanying amplificationin band intensity as a function of increasing amounts of HRSFextract added to the incubation mixture. **1B, TEM analysis** depicting shape and size of as-synthesized AgNPs, of the size dimensions of 10-40 nm, prepared with less (3 ml) HRSF extract, **1C**, **Representative TEM image** of as-formed silver nanoparticles, of the size dimensions of 15-25 nm, synthesized employing relatively high (5 ml) HRSF extract. TEM micrograph depicts presence of various shaped nanostructures ofAgNPs with size dimensions in the range of 30-50 nm. **1D,Dynamic Light Scattering Size analysis** of the AgNPs: Particle size analysis with DLS (Dynamic Light Scattering) suggests overall particle radii of the as-synthesized silver nanoparticles to be approximately in the range of 30–80 nm. **1E, Zeta potential analysis** of the as-formed AgNPs. The as-synthesized AgNPs were analyzed for their surface charge employing Zeta sizer (Malvern Instrument Ltd., UK) as described in method section. The zeta potential of as-synthesized AgNPs was found out to be around -25 mV.

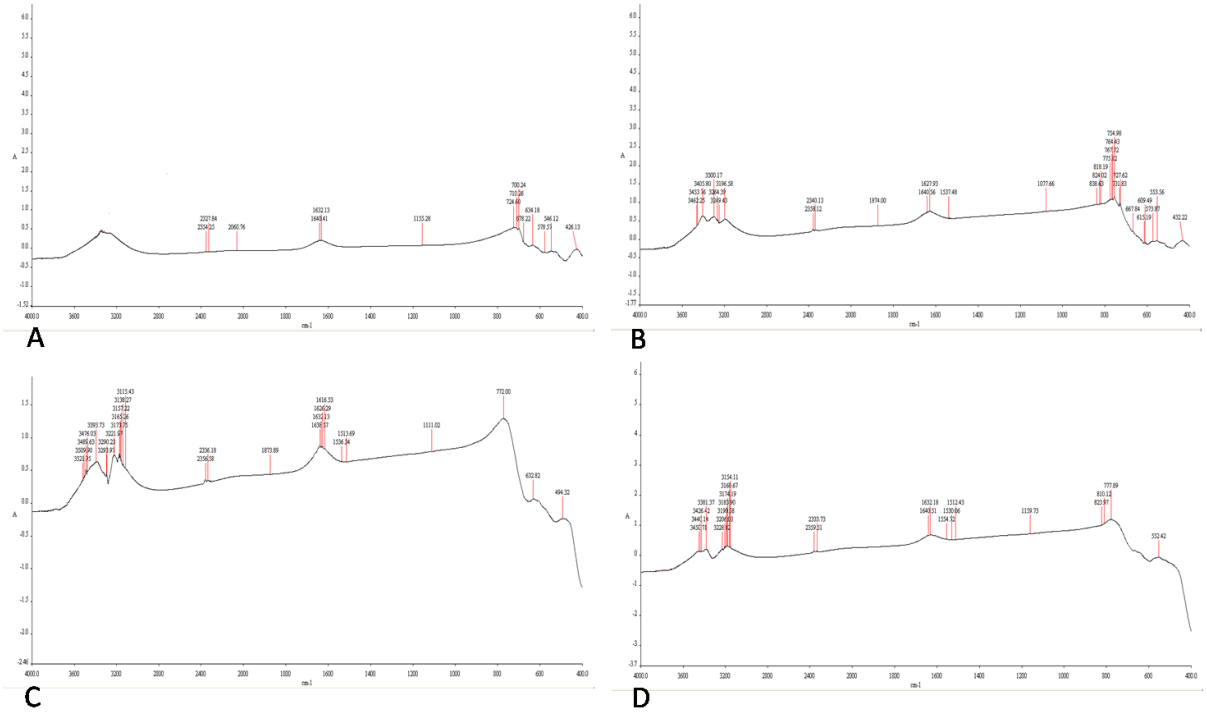

Figure 2

Figure 2. FTIR spectrum of as-formed AgNPs. FTIR spectrophotometry was used for characterization of resultant silver nanoparticles obtained after HRSF extract mediated reduction of silver nitrate.FTIR spectra of flower extract and silver nanoparticles generated

Preprints (www.preprints.org) | NOT PEER-REVIEWED | Posted: 19 February 2021 doi:10.20944/preprints202102.0436.v1

after adding 3ml and 5ml of extact into the aqueous solution of $AgNO_3$. Curve A, represenative of pure *Hibiscus* flower extract, curve B of aqueous solution of pure $AgNO_3$, curves C and D correspond to silver nanoparticles synthesized by the reduction of chloroauric acid with addition of 3ml and 5ml of flower extract respectively.

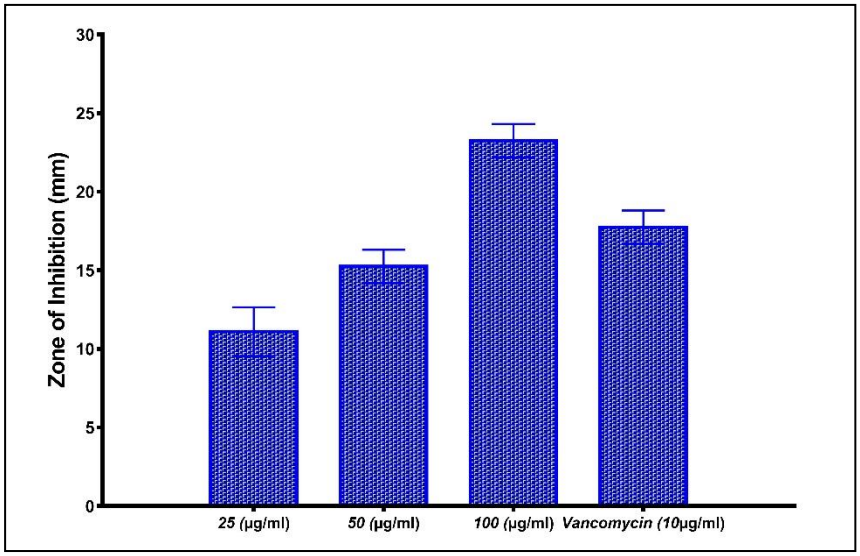

Figure 3

Figure 3.Antimicrobial potential of as-synthesized AgNPs. The antimicrobial property of the as-synthesized AgNPs was expressed in terms of the zone of inhibition (in mm) using vancomycin as standard antibiotic. The as-synthesized AgNPs were found to be effective against *S. mutans* bacteria in dose dependant manner.

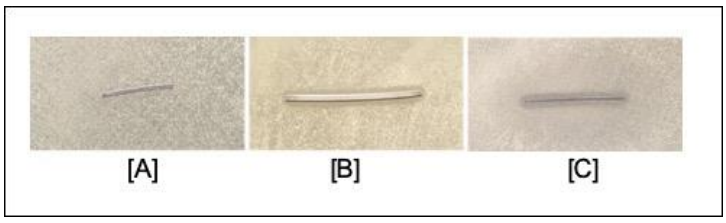

Figure 4

Figure 4. Anti-Bacterial potential of AgNPs coated Ni-Ti orthodontic wire. A). Control. Uncoated Ni-Ti orthodontic wire. B) Orthodontic wire incubated with $AgNO_3$ solution. C) Orthodontic wire adsorbed with as-synthesized AgNPs.

Preprints (www.preprints.org) | NOT PEER-REVIEWED | Posted: 19 February 2021 doi:10.20944/preprints202102.0436.v1

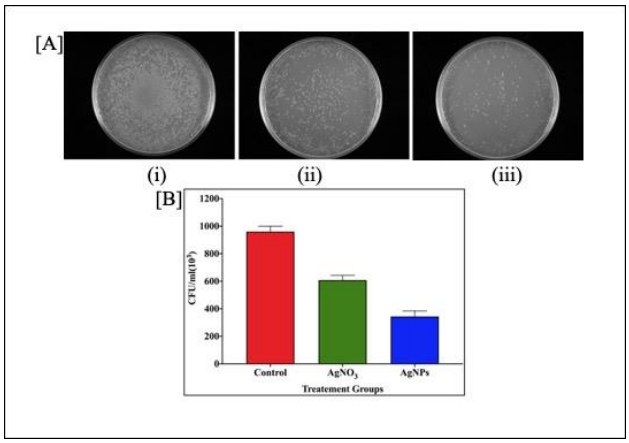

Figure 5

Figure 5a. Anti-adherence properties of AgNPs coated orthodontic wires. Adhered *S. mutans* bacterial population collected from: A) uncoated orthodontic wire, B) wire incubated with $AgNO_3$ solution, and C) wire adsorbed with as-synthesized AgNPs.

Figure 5b.Anti-adherence property of AgNPs impregnated Ni-Ti orthodontic wires. The bacterial burden in terms of CFU corresponding to adhered bacterial population present on the surface of Ni-Ti orthodontic wire: Control- uncoated Ni-Ti orthodontic wire, (B) Silver nitrate (aqueous solution) coated Ni-Ti orthodontic wire (C) Ni-Ti orthodontic wire coated with as-synthesized AgNPs.

Preprints (www.preprints.org) | NOT PEER-REVIEWED | Posted: 19 February 2021 doi:10.20944/preprints202102.0436.v1

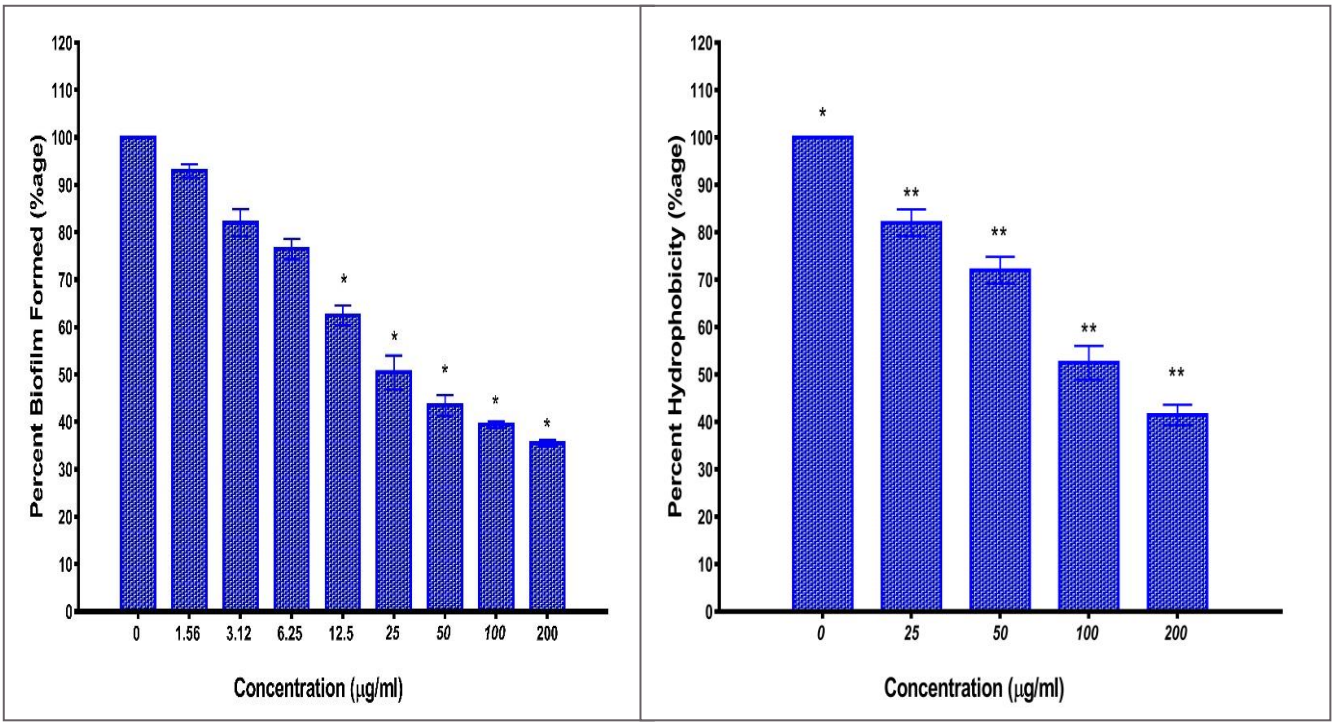

[A
1

[B]

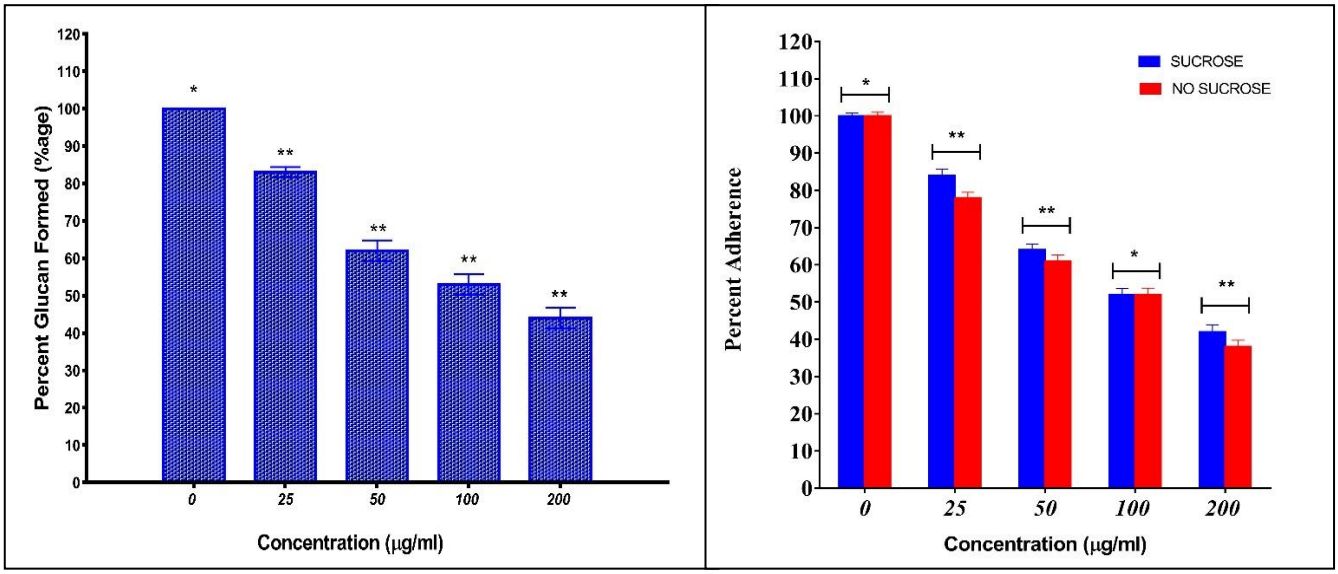

[C]

[D]

Figure 6

Figure 6. Anti-biofilm potential of as-synthesized AgNPs. The anti-biofilm property of as-synthesized AgNPs against *S. mutans* as revealed by employing A) XTT assay and B) Hydrophobicity assay. As-synthesized AgNPs were able to inhibit glucan synthesis by *S.*

Preprints (www.preprints.org) | NOT PEER-REVIEWED | Posted: 19 February 2021 doi:10.20944/preprints202102.0436.v1

mutans(C) as well as also resulted in its decreased adherence potential on glass surface (D). [*: P value < 0.001, **: P value < 0.005]

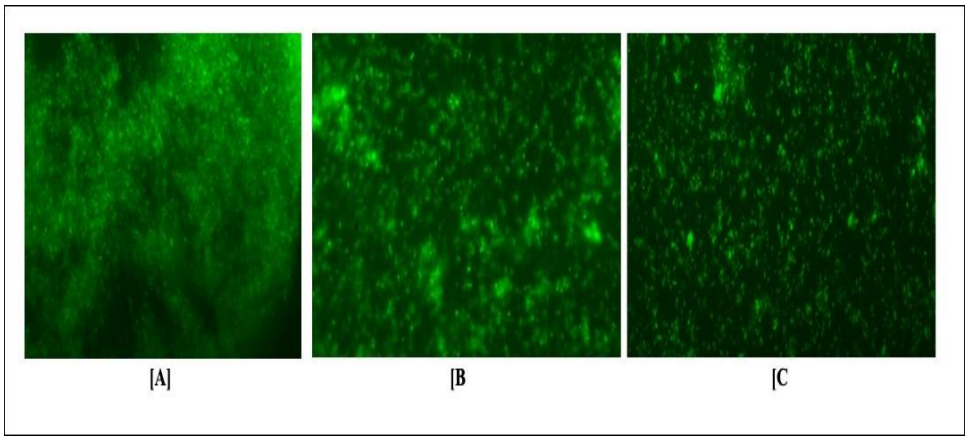

Figure 7

Figure 7. As-synthesized AgNPs inhibit *S. mutans* biofilm as revealed by fluorescence microscopy. A) Mature, untreated biofilm of *S. mutans*, B) biofilm inhibition upon treatment with $AgNO_3$ solution, C) biofilm inhibition upon treatment with as-synthesized AgNPs.

Preprints (www.preprints.org) | NOT PEER-REVIEWED | Posted: 19 February 2021 doi:10.20944/preprints202102.0436.v1

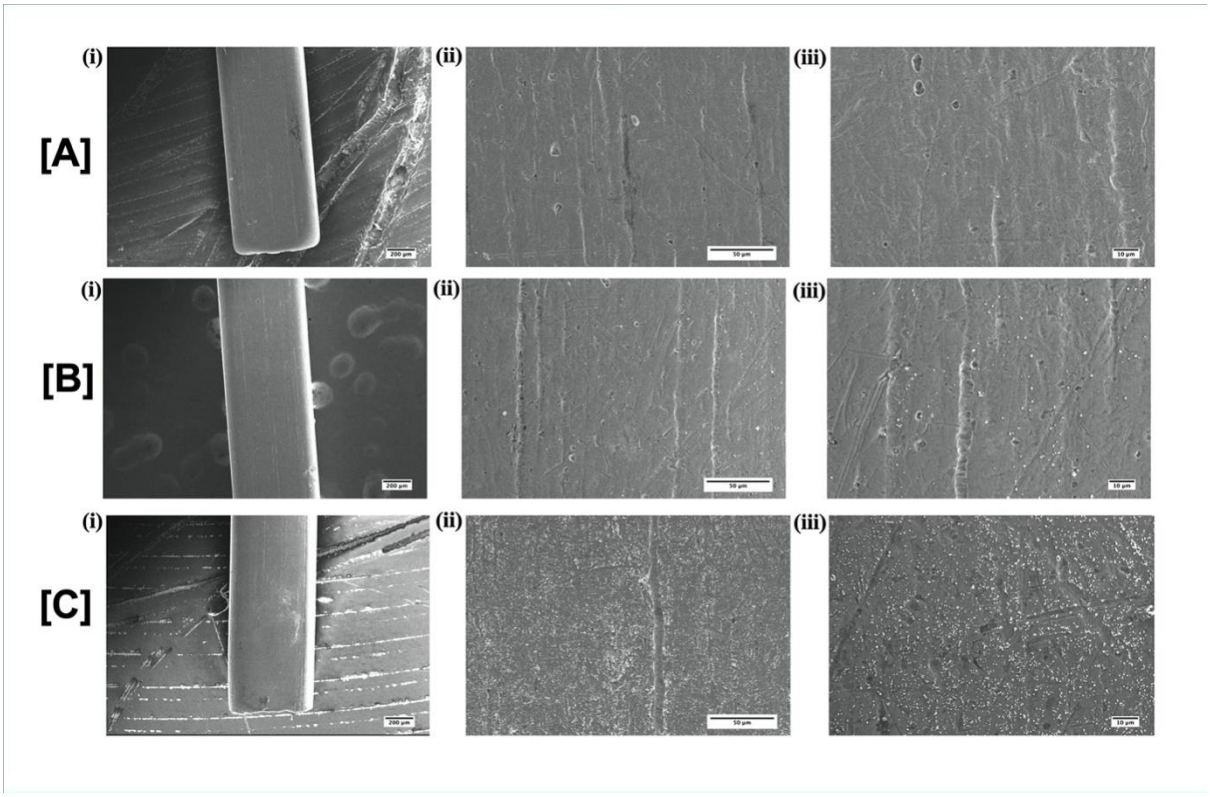

Figure 8

Figure 8. Surface characterization of AgNPs coated Ni- Ti orthodontic wire. Scanning Electron Micrographs showing graded magnifications of: A) uncoated wire, B) wire coated with aqueous $AgNO_3$ solution. (C) wire coated with as-synthesized AgNPs

4. Discussion

Recent upsurge in the emergence of microbial isolates, which can withstand antibiotic onslaught, has inflicted serious impact on the strategies employed in the treatment of various infectious diseases. The failure of antibiotics in killing disease causing microbes calls for development of alternate mode of therapy. The survival of pathogenic microbes in the oral cavity depends on their successful adhesion to dental surfaces and their ability to develop into biofilms. The as-formed biofilm protects microbes from environmental challenges and help in their growth and propagation. The microbial biofilm can develop on dental implants leading to peri-implantitis that is considered to be the main reason for implant failure.

Interestingly, metal-based nano-particles offer a salvage strategy to treat oral infection. In this regard, silver based nanoparticles (AgNPs) can successfully control infection [18]. Moreover, synthesis of nanoparticles employing biological methods i.e. green synthesis offers additional

Preprints (www.preprints.org) | NOT PEER-REVIEWED | Posted: 19 February 2021 doi:10.20944/preprints202102.0436.v1

benefits in terms of biocompatibility and bioavailability. Hence, we explored HRFS based extract for its potential to synthesize AgNPs. Next, we examined the antibacterial and anti-adherence activity of as-synthesized AgNPs on the surface of Ni- Ti orthodontic wires against *S. mutans*.

To begin with, first we characterized as-synthesized AgNPs for their physico-chemical attributes. To track the crystallization progress, TEM and UV spectro-photometric studies were carried out. The *HRSF* mediated biological synthesis lead to formation of spherical AgNPs, with size distribution in the range of 15-40 nms. The DLS analysis suggested the size dimension of as-synthesized AgNPs in the range of 30-80 nm. The discrepancy in the observed average size of the as-synthesized particles can be attributed to the method used in the size determination (19).

The as-synthesized AgNPs were found to exhibit characteristic SPR showing absorption peak in the range of 480nm. In accordance with Mie theory, a single SPR band is obtained in case of spherical nanoparticles. The FT-IR spectroscopy also suggested formation of a new micro-ambience corresponding to functional groups of the parent compounds present in HRS flower extract.

The zeta potential values ranging from +30 to -30 mV are supposed to help in maintaining the stability of the related nanoparticles [20]. Incidentally the as-synthesized AgNPs were found to have zeta potential around -35 mV. This suggests that HRSF extract mediate synthesis of stable AgNPs.

Keeping into consideration usefulness of silver nanoparticles in treatment of range of microbes, we tested their anti-biofilm potential against various other classes of bacteria in addition to *S. mutans*. We made an elaborated effort to ascertain the effect of as-synthesized AgNPs against both resistant as well sensitive bacterial isolates. The anti-biofilm activity, as revealed by XTT assay, suggests that as-synthesized AgNPs can significantly inhibit less susceptible isolates of *S. mutans, E. coli and L. monocytogenes*. The observed effectiveness of as-synthesized AgNPs to kill both sensitive as well as less susceptible isolates of bacteria has great relevance in the present scenario where drug resistance crisis by microbes is posing great health concern. Moreover, as-synthesized AgNPs were also shown to inhibit glucan synthesis by *S. mutans*.

Preprints (www.preprints.org) | NOT PEER-REVIEWED | Posted: 19 February 2021 doi:10.20944/preprints202102.0436.v1

We established potential of Ag NPs to inhibit bacterial growth on orthodontic appliances. The AgNPs deposited onto the surface of experimental dental appliances including orthodontic wire showed strong antimicrobial properties. In general, orthodontic appliances serve as a favorable site for *S. mutans* to adhere, by forming a bacterial biofilm on their surface. However, if coated with AgNPs, they showed significant anti-adherence properties as well. The electron microscopic studies further established anti-adherence activity of the AgNPs on orthodontic wires (Figure 8).

While practice of establishing antimicrobial activity of AgNPs against various pathogens is a common feature, the studies pertaining to anti-adherence potential of AgNPs in context of orthodontic wires are limited [21]. This makes the present approach more relevant as we have demonstrated that coating of AgNPs on to the surface of orthodontic wire impart anti-adherence properties to the later. This observation is very interesting and has a great relevance as orthodontic wire and other related dental appliances are very prone to be contaminated by various oral bacteria including *S. mutans*.

Earlier studies have suggested that AgNPs have the ability to release silver ions that have potential to kill target bacterial cells [22]. The observed anti-adherence property of the AgNPs may be attributed to the fact that they can penetrate the cell wall of associated bacteria and also prevent production of extracellular polysaccharide to check bacterial adhesion on orthodontic wire.

The immersion of orthodontic wire in AgNPs suspension followed by their interaction with *S. mutans* on the agar plate ensued in killing (clear zone of inhibition) of bacteria present in the surrounding ambiance. There is a possibility that AgNPs may interact with thiol or amino residues of various crucial enzymes and eventually lead to inhibition of the bacterial cells [23]. The large surface area of as-formed AgNPs is likely to facilitate inhibition of various metabolically active enzymes. Moreover, AgNPs have also been reported to facilitate generation of reactive oxygen species under oxygen atmosphere [24]. The potential of as-generated ROS to act on proteins and DNA based macromolecules has been considered detrimental to the live bacterial cells [25]. The higher adhesion of *S. mutans* can be attributed to the surface morphology of the uncoated (bare) orthodontic wires [Figure 4]. The rougher surfaces are known to encourage biofilm formation and support greater adherence. In contrast, the treatment with AgNPs minimizes irregular cavities and undulating surface of orthodontic wires, thereby minimizes adherence of *S. mutans* (Figures 4 & 8).

Finally, we can conclude that as-formed AgNPs showed remarkable antibacterial potential against both resistant as well as sensitive isolates of the bacteria. The adsorption of as-synthesized AgNPs on orthodontic wire imparts strong antibacterial attributes to the Ni-Ti orthodontic wires. We speculate that AgNP impregnated, orthodontic wires acquire intrinsic potential to inhibit bacterial growth upon their use in clinical setting.

Acknowledgement. The authors express their gratitude to the Co-Ordinator, Interdisciplinary Biotechnology Unit, Aligarh Muslim University, Aligarh for providing facilities to complete this study. We are thankful to AAM for his help in drafting of the manuscript.

Authors Contribution. SF and MO conceived and designed the experiments. SF, NK, AMO MSU, AWA and FJ performed the experiments. SF, MK and NK analyzed the data. MO and SK contributed the reagents/materials/analysis tools.

Competing Financial Interest. Authors declare there is no conflict of interest.

References

1. Guerrero-Martínez, A., Pérez-Juste, J. and Liz-Marzán, L.M., 2010. Recent progress on silica coating of nanoparticles and related nanomaterials. *Advanced materials*, *22*(11), pp.1182-1195.
2. Abbasi, E., Milani, M., Fekri Aval, S., Kouhi, M., Akbarzadeh, A., TayefiNasrabadi, H., Nikasa, P., Joo, S.W., Hanifehpour, Y., Nejati-Koshki, K. and Samiei, M., 2016. Silver nanoparticles: synthesis methods, bio-applications and properties. *Critical reviews in microbiology*, *42*(2), pp.173-180.
3. Buzea, C., Pacheco, I.I. and Robbie, K., 2007. Nanomaterials and nanoparticles: sources and toxicity. *Biointerphases*, *2*(4), pp.MR17-MR71.
4. Petros, R.A. and DeSimone, J.M., 2010. Strategies in the design of nanoparticles for therapeutic applications. *Nature reviews Drug discovery*, *9*(8), pp.615-627.
5. Vashist, A., Vashist, A., Gupta, Y.K. and Ahmad, S., 2014. Recent advances in hydrogel based drug delivery systems for the human body. *Journal of Materials Chemistry B*, *2*(2), pp.147-166.

6. Loo, Y.Y., Chieng, B.W., Nishibuchi, M. and Radu, S., 2012. Synthesis of silver nanoparticles by using tea leaf extract from Camellia sinensis. *International journal of nanomedicine*, *7*, p.4263.
7. Bhosale, R.R., Kulkarni, A.S., Gilda, S.S., Aloorkar, N.H., Osmani, R.A. and Harkare, B.R., 2014. Innovative eco-friendly approaches for green synthesis of silver nanoparticles. *Int J Pharm Sci Nanotech*, *7*(1), pp.2328-2337.
8. Ramya, M. and Subapriya, M.S., 2012. Green synthesis of silver nanoparticles. *Int J Pharm Med Biol Sci*, *1*(1), pp.54-61.
9. Ritter, A.V., Eidson, R.S. and Donovan, T.E., 2014. Dental caries: etiology, clinical characteristics, risk assessment, and management. *Sturdevant's Art & Science of Operative Dentistry-E-Book*, *41*.
10. Lekhadia, D.R., 2018. Nanotechnology in Orthodontics—Futuristic Approach. In *Dental Applications of Nanotechnology* (pp. 155-175). Springer, Cham.
11. Socransky, S.S. and Haffajee, A.D., 2002. Dental biofilms: difficult therapeutic targets. *Periodontology 2000*, *28*(1), pp.12-55.
12. Durack, D.T., Gilliland, B.C. and Petersdorf, R.G., 1978. Effect of immunization on susceptibility to experimental Streptococcus mutans and Streptococcus sanguis endocarditis. *Infection and immunity*, *22*(1), pp.52-56.
13. Gallardo, C.M.C., Hernandez, S.A.C., Lopez, L.F.M. and Rojas, J.P.G., Universidad de Chile, 2019. *Preparation process of dental and orthopedic acrylic materials with antimicrobial properties using copper nanoparticle technology*. U.S. Patent Application 16/067,053.
14. Lim, T.K., 2014. Hibiscus rosa-sinensis. In *Edible Medicinal and Non Medicinal Plants* (pp. 306-323). Springer, Dordrecht.
15. Shewale, P.B., Patil, R.A. and Hiray, Y.A., 2012. Antidepressant-like activity of anthocyanidins from Hibiscus rosa-sinensis flowers in tail suspension test and forced swim test. *Indian journal of pharmacology*, *44*(4), p.454.
16. Farkas, K., Varsani, A. and Pang, L., 2015. Adsorption of rotavirus, MS2 bacteriophage and surface-modified silica nanoparticles to hydrophobic matter. *Food and environmental virology*, *7*(3), pp.261-268.
17. Dutta, D., Sahoo, A.K., Chattopadhyay, A. and Ghosh, S.S., 2016. Bimetallic silver nanoparticle–gold nanocluster embedded composite nanoparticles for cancer theranostics. *Journal of Materials Chemistry B*, *4*(4), pp.793-800.

18. Wang, L., Hu, C. and Shao, L., 2017. The antimicrobial activity of nanoparticles: present situation and prospects for the future. *International journal of nanomedicine*, *12*, p.1227.
19. Mourdikoudis S, Pallares RM, Thanh NT. Characterization techniques for nanoparticles: comparison and complementarity upon studying nanoparticle properties. Nanoscale. 2018;10(27):12871-934.
20. Sun, Q., Cai, X., Li, J., Zheng, M., Chen, Z. and Yu, C.P., 2014. Green synthesis of silver nanoparticles using tea leaf extract and evaluation of their stability and antibacterial activity. *Colloids and surfaces A: Physicochemical and Engineering aspects*, *444*, pp.226-231.
21. Francolini, I., Vuotto, C., Piozzi, A. and Donelli, G., 2017. Antifouling and antimicrobial biomaterials: an overview. *Apmis*, *125*(4), pp.392-417.
22. Mohanty, S., Mishra, S., Jena, P., Jacob, B., Sarkar, B. and Sonawane, A., 2012. An investigation on the antibacterial, cytotoxic, and antibiofilm efficacy of starch-stabilized silver nanoparticles. *Nanomedicine: Nanotechnology, Biology and Medicine*, *8*(6), pp.916-924.
23. Rizzello, L. and Pompa, P.P., 2014. Nanosilver-based antibacterial drugs and devices: mechanisms, methodological drawbacks, and guidelines. *Chemical Society Reviews*, *43*(5), pp.1501-1518.
24. Li, Y., Zhang, W., Niu, J. and Chen, Y., 2013. Surface-coating-dependent dissolution, aggregation, and reactive oxygen species (ROS) generation of silver nanoparticles under different irradiation conditions. *Environmental science & technology*, *47*(18), pp.10293-10301.
25. Zheng, K., Setyawati, M.I., Leong, D.T. and Xie, J., 2018. Antimicrobial silver nanomaterials. *Coordination Chemistry Reviews*, *357*, pp.1-17.